Earth and Planetary Science Letters 309 (2011) 141–152

Contents lists available at ScienceDirect

Earth and Planetary Science Letters

journal homepage: www.elsevier.com/locate/epsl

Magnetic properties as tracers for source-to-sink dispersal of sediments: A case study in the Taiwan Strait

Chorng-Shern Horng *, Chih-An Huh

Institute of Earth Sciences, Academia Sinica, P. O. Box 1–55, Nankang, Taipei 11529, Taiwan, ROC

ARTICLE INFO

Article history:
Received 11 February 2011
Received in revised form 28 June 2011
Accepted 4 July 2011
Available online 29 July 2011

Editor: P. DeMenocal

Keywords:
magnetic properties
pyrrhotite
magnetite
source-to-sink systems
sediments
Taiwan Strait

ABSTRACT

Different lithologies between Taiwan and southeastern China lead to diverse mineralogical composition for weathering products derived from the two shores of the Taiwan Strait. Pyrrhotite and magnetite are respectively the dominant magnetic minerals associated with fluvial sediments from western Taiwan and southeastern China. While magnetite commonly co-exists with pyrrhotite in sediments sourced from Taiwan, pyrrhotite has not been found in sediments sourced from mainland China. Associated with such a distinction are vast differences in magnetic properties, including magnetic susceptibility (χ), SIRM, HIRM and the S-ratio, which can be used to study the provenances of sediments in the Taiwan Strait and adjoining marginal seas. Based on any two of these parameters, the magnetic characteristics of much of the Taiwan Strait sediment can be explained using a two-endmember mixing model. Source-to-sink dispersal of sediments in the Taiwan Strait can then be traced from the distribution of these parameters. The results not only corroborate an earlier study based on radionuclides and particle size distribution (Huh et al., 2011) but reveal more diagnostic details.

Besides spatial distribution based on a large number (216) of surface sediments, we also analyzed temporal variation of magnetic properties in six well-dated cores collected at key sites along the sediment source-to-sink pathways. From profiles of these parameters in cores from the middle of the northern Taiwan Strait, it is calculated that sediment supply from Taiwan has increased substantially in the past five decades, which may very well be related to accelerated land use and increased frequency of intense rainfalls in Taiwan during the same period.

The approach described in this work may be extended to other source-to-sink systems around the world and through time, especially the mountainous islands fringing the Pacific and Indian Oceans in southeastern Asia. As with Taiwan, these islands have high denudation rates and pyrrhotite is in all likelihood a mineral characteristic of their metamorphic terrains.

1. Introduction

The Taiwan Strait (TS) is located between Taiwan, the Asian continent, the South China Sea (SCS) and the East China Sea (ECS) (Fig. 1a). Covering an area of ~63,000 km^2 with a mean water depth of 60 m, the strait connects two largest marginal seas in the western Pacific and collects sediments removed from the world's largest land mass in its west and a mountainous island with the highest erosion rate in its east (Dadson et al., 2003; Huh et al., 2009; Li, 1976). It is thus quite conceivable that the transport of sediment and flow of water through this relatively narrow and shallow, but all-important passage must be very massive and dynamic.

Sediments in the TS are mainly delivered from western Taiwan and southeastern China by rivers draining catchment basins with very different lithologies. Western Taiwan rivers are sourced either from mountainous (>3000 m) metamorphic terrains exhumed during the Plio–Pleistocene orogeny, or from sedimentary terrains in the foothills on the west of the metamorphic mountain ranges (Chen et al., 2000; Fig. 1b). Together, these rivers contribute most of their sediment loads, ~153×10^6 ton/yr, to the TS (WRB, 1998), which is equivalent to the sediment load of the Yangtze River (Yang et al., 2002, 2003) whose drainage basin occupies an area ~100 times that of western Taiwan. In comparison with Taiwan's small mountainous rivers running through steep topography, rivers in southeastern China flow over large and flat drainage basins mainly underlain by Jurassic–Cretaceous igneous rocks (Ma, 2002). Most of these large rivers' sediment loads are accumulated at their subaqueous prodelta or the alongshore clinoform, with a relatively small fraction reaching the TS (Liu et al., 2007, 2008; Xu et al., 2009).

The geological and geomorphic backdrop described above results in fluvial sediments with distinct properties characteristic of their respective provenances, thus providing diagnostic tracers to investigate

* Corresponding author.
E-mail addresses: cshorng@earth.sinica.edu.tw (C.-S. Horng), huh@earth.sinica.edu.tw (C.-A. Huh).

0012-821X/$ – see front matter © 2011 Elsevier B.V. All rights reserved.
doi:10.1016/j.epsl.2011.07.002

fates of detrital sediments from a source-to-sink perspective. Huh et al. (2011) used radionuclides (^{210}Pb, ^{137}Cs, ^{7}Be and ^{234}Th) as tracers to elucidate the sources, pathways and accumulation rates of sediments in the TS. They outlined three different sediment source-to-sink dispersal systems that are closely related to hydrodynamics in the TS (see next section). Alternatively, sediment magnetic properties offer another approach to this issue using simple, rapid and nondestructive rock magnetic method that have been widely applied to Earth's surface

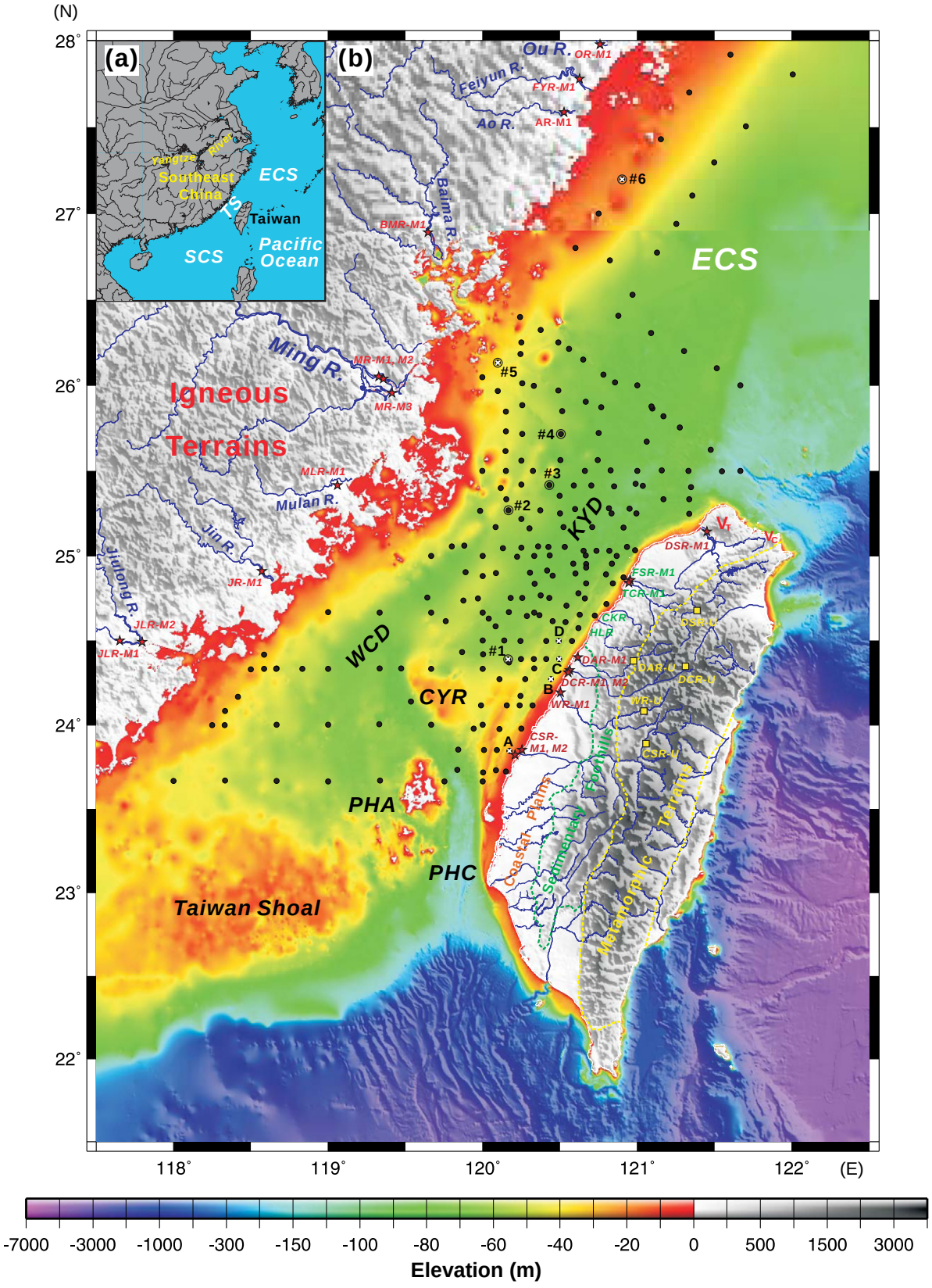

process and environmental studies (Evans and Heller, 2003; Maher and Thompson, 1999; Thompson and Oldfield, 1986). In this work, we analyzed magnetic properties of sediments from the TS and western Taiwan and southeastern China rivers, and used them as proxies for concentration, composition, and grain size of magnetic minerals to identify provenances of sediments in the strait. X-ray diffraction (XRD) analysis and scanning electron microscopic (SEM) observations were also made on magnetic extracts from the sediments to corroborate our interpretation of the magnetic properties.

2. The oceanographic setting

The bathymetry of the Taiwan Strait (Fig. 1b) is characterized by several salient features as follows. The Penghu Channel (PHC) in the southeast is the deepest region of the strait. Shallow waters are distributed in the Taiwan Shoal and the Penghu Archipelago (PHA) in the west of the PHC and over the Chang-Yun Ridge (CYR) in the middle reaches of the TS. The Kuan-Yin Depression (KYD) in the northeast and the Wu-Chiu Depression (WCD) in the west are two major basins separated by the CYR; collectively these two basins account for much of the strait's area.

The funnel-shaped PHC is the most important gateway through which the Kuroshio Branch Current (KBC) derived from the Luzon Strait flows into the TS (Jan et al., 2002). As the year-round KBC (plus the SCS Current in the summer and fall seasons) is funneled through the PHC, the northbound current bifurcates in front of the CYR, with a deeper component turning northwestward around the western CYR and a shallow component crossing the swale between the eastern CYR and the western CYR (Fig. 2; also see Fig. 2 in Liao et al., 2008). The deep, western branch of KBC then flows along the eastern edge of the WCD, turning northeastward into the KYD at ~24.5°N to merge with the shallow, eastern branch of KBC behind the CYR. This combined current, commonly referred to as the Taiwan Warm Current (TWC), flows over the KYD and exits the TS in its north. The volume transport of TWC is the largest at the peak of the summer (southwest) monsoon and the lowest at the peak of the winter (northeast) monsoon (Jan et al., 2006).

On the western side of the strait flows the southbound China Coastal Current (CCC). Since the CCC and the TWC flow in opposite directions, their waxing and waning are therefore opposite to each other in response to the annual cycle of summer and winter monsoons. When the southwest monsoon peaks in the summer, the CCC is virtually nonexistent in the TS (Fig. 2c). Conversely, when the northeast monsoon prevails in the wintertime (Fig. 2a), the CCC may extend southward to the middle reaches of the TS, with a part obstructed by the CYR and turning back northward to form a cyclonic eddy in the KYD (Jan et al., 2002, 2004; Lee and Chao, 2003; Wu et al., 2007).

Besides circulation of water masses (i.e., mean current flows) at greater spatial and temporal scales, tidal currents also play an important role in the hydrodynamics as well as sedimentation dynamics in estuarine, coastal and shelf environments. Among tides of various frequencies, the semidiurnal M_2 tide is by far the most predominant one in the TS (Jan et al., 2004; Wang et al., 2003). Fig. 3 shows M_2 tidal current ellipses in the TS derived by Wang et al. (2003) based on shipboard ADCP (Acoustic Doppler Current Profiler) observations during 1999–2001. In the eastern TS, the motions of M_2 tides are generally alongshore and of reversing-type, with the strongest flows found along the PHC and off the northwestern coast of Taiwan; from there the sizes of M_2 tidal current ellipses decrease while the tidal levels increase toward the middle of the TS (Huh et al., 2011). In the western side of the TS, especially the northwestern sector of the strait, the tidal ellipses are more rounded than those in the eastern TS, reflecting rotating-type motions which are more favorable for trapping fine sediments.

3. Materials and methods

A total of 216 marine surface (<2 cm) sediments taken from the top of box or gravity cores and 157 samples sectioned at 2-cm intervals from 6 well-dated cores were used for this study. Before conducting magnetic measurements, these samples had already been dried and nondestructively analyzed for a series of radionuclides including ^{137}Cs and ^{210}Pb as sediment chronometers (Huh et al., 2011). In order to identify the sources of Taiwan Strait sediments, 25 fluvial sediments from main rivers in western Taiwan and southeastern China were also collected and analyzed. Among them, 5 samples are located in the upper reaches of western Taiwan rivers where the metamorphic bedrocks are incised, and the rest are near the mouths of rivers where the sediments represent an integration of materials (soils and rock debris) removed from the entire drainage basins. Locations of all these sediments are indicated in Fig. 1.

To minimize the effect of grain size on the measurements of magnetic properties and to exclude the interference from large shell fragments, all the samples were sieved using a 63-μm net to collect mud (i.e., silt and clay-sized particles), which is the dominant fraction for most (>80%) of the samples. Less than 40 surface samples were dominated by coarse grains (larger than very fine sands, >63 μm), which were sieved sequentially using 63-μm, 125-μm and 250-μm nets. In order to express magnetic parameters in mass-normalized terms, ~8 g of sieved sediments was transferred to a ~7-cm^3 plastic cube for each specimen and weighed with a precision of 0.1 mg. The magnetic susceptibility (χ) of all cubic specimens was measured in a low magnetic field with a Bartington Instruments MS2B magnetic susceptibility meter. Then, using a 2G Enterprises triaxial degausser, anhysteretic remanent magnetizations (ARMs) were imparted along the z-axis of the specimens in a 0.05 mT direct current (DC) bias field with a maximum peak alternating field of 90 mT. ARMs were then measured with a 2G Enterprises superconducting rock magnetometer and values of ARM susceptibility (χ_{arm}) were obtained by dividing ARM with the DC bias field. Subsequently, saturation isothermal remanent magnetizations (SIRMs) were imparted along the specimen z-axis using a DC field of 2 T generated using a Magnetic Measurements Ltd. pulse magnetizer. After measuring the SIRMs, a reversed DC field of 0.3 T was applied to the specimens for measurements of this magnetization, defined as $IRM_{-0.3T}$, using the same rock magnetometer. S-ratios and hard isothermal remanent magnetizations (HIRMs) were then calculated following the definitions of King and Channell (1991); i.e., S-ratio = $(-IRM_{-0.3T}/SIRM)\times 100\%$, and HIRM = $(IRM_{-0.3T}+SIRM)/2$.

As an all-important magnetic parameter, χ is effectively a measure of the concentration of ferrimagnetic minerals (essentially magnetite) in

Fig. 1. Map showing (a) the location of the Taiwan Strait (TS), which connects the East China Sea (ECS) and the South China Sea (SCS), (b) the bathymetry of the Taiwan Strait and rivers on its both sides. Major topographic features in the strait are Penghu Channel (PHC), Penghu Archipelago (PHA), Chang-Yun Ridge (CYR), Kuan-Yin Depression (KYD), Wu-Chiu Depression (WCD) and Taiwan Shoal. Major western Taiwan rivers discharging directly into the strait include (from north to south): Danshui (DSR), Fengshan (FSR), Touchien (TCR), Chungkang (CKR), Houlong (HLR), Daan (DAR), Dachia (DCR), Wu (WR), and Choshui (CSR) Rivers. Among these rivers, Danshui, Daan, Dachia, Wu and Choshui Rivers are derived from mountainous metamorphic terrains (i.e., the region enclosed by the yellow dashed lines) and others are from the sedimentary western foothills (i.e., the area between the green and yellow dashed lines). By contrast, the Ou, Ming and other Rivers in southeastern China flow through igneous terrains. Dots (●) denote locations of 216 surface sediments in the TS. Circled dots (◉) represent sites (#1–#6) where cored sediments were well-dated for this study. Crossed dots (⊗) mark sites (A–D, #1, #5 and #6) where magnetic minerals were extracted from the samples for XRD and SEM analyses (see Figs. 4–5). Squares are sites where fluvial sediments were collected from the upper reaches of five western Taiwan rivers sourced from the metamorphic terrains. Stars show sampling sites near the mouths of western Taiwan and southeastern China rivers. Locations of the Tatun and Chilung Volcano Groups in northern Taiwan are indicated by V_T and V_C, respectively.

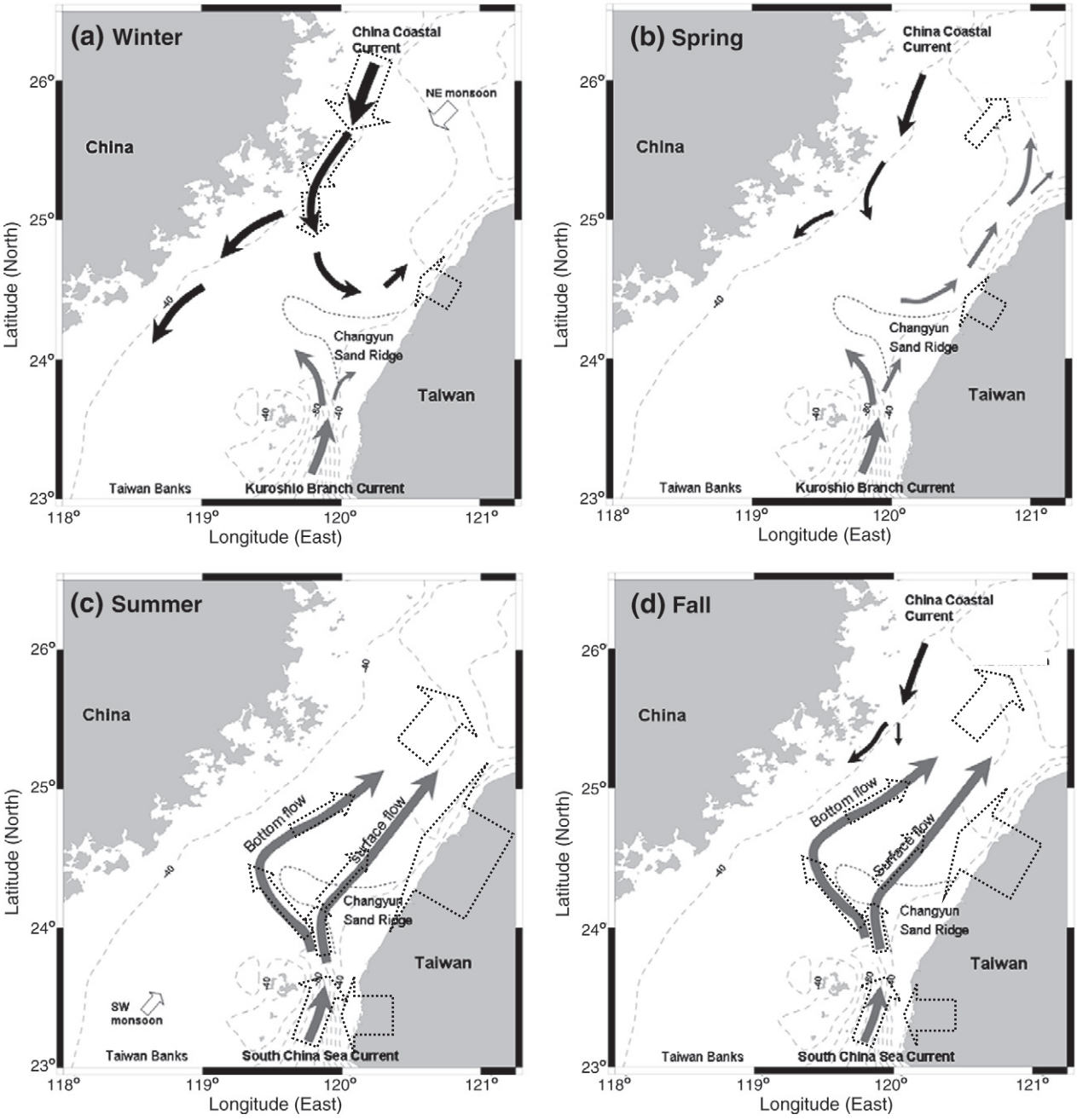

Fig. 2. Seasonal circulation patterns in the Taiwan Strait, with water flows indicated by solid arrows and sediment transport indicated by dotted arrows. Redrawn from Jan et al. (2002).

the samples. The ARM susceptibility (χ_{arm}) is also a useful parameter in its own right and it preferentially responds to single-domain (SD) magnetic particles. The χ_{arm}/χ ratio can be used to distinguish particle size of sediments in general and magnetic minerals in particular (Banerjee et al., 1981). SIRM is highly dependent on the make-up of different types of magnetic minerals (e.g., magnetite has measurements two orders of magnitude higher than hematite). The S-ratio provides a fair estimate of the relative contribution of antiferromagnetic minerals (e.g., hematite) versus ferrimagnetic minerals (e.g., magnetite) to the remanence. HIRMs can be used as measures of the absolute amounts of "hard" magnetic minerals, such as hematite and goethite. From a properly combined use of these magnetic parameters, it is possible to discriminate concentrations, grain sizes and types among the main magnetic minerals in natural samples (Oldfield, 1999).

To corroborate the interpretation based on magnetic parameters, magnetic minerals were extracted from selected surface sediments using a rare earth magnet housed in a plastic sheath. XRD analysis was then carried out on magnetic extracts using a Rikagu Miniflex table top unit (Cu-Kα radiation). The X-ray scans were run from 4° to 80° (2θ). Results are presented after subtraction of the background trend. Following the XRD analysis, observations of magnetic extracts were made using a JOEL JSM-6360LV SEM operated at 15 keV with 18 nA acceleration voltage. Chemical spectra of minerals were obtained using an Oxford Instruments Ltd. INCA-300 X-ray energy dispersive spectrometer (EDS).

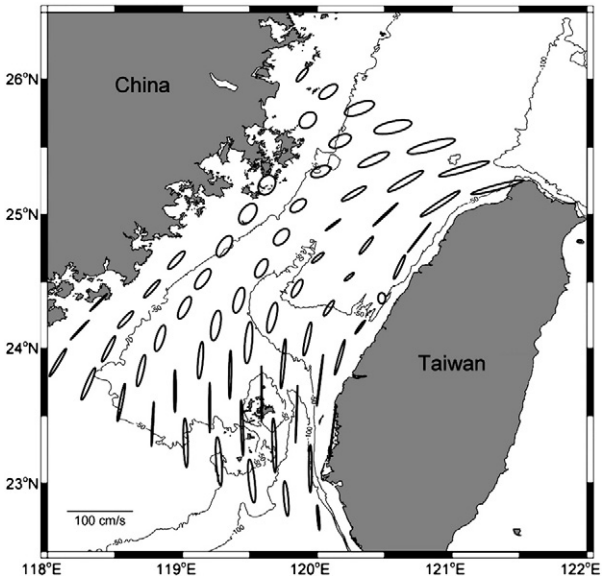

Fig. 3. M_2 tide ellipses in the Taiwan Strait. Redrawn from Wang et al. (2003).

4. Results and discussion

4.1. Major magnetic minerals from XRD and SEM observations

Shown in Fig. 4 are X-ray diffractograms of magnetic extracts from surface sediments collected from six key sites; five are located near the mouths of representative rivers from opposite sides of the Taiwan Strait (i.e., the Choshui, Wu and Dachia Rivers of western Taiwan and the Ming and Ou Rivers of southeastern China) and one is in the south of the Kuan-Yin Depression (see Fig. 1 for their locations). It is clear that, accompanied by a very small amount of hematite, magnetite is the dominant and omnipresent magnetic mineral in sediments not only near the Ou and the Ming Rivers' estuaries (Fig. 4a–b) but also in the Yangtze River's estuary and the East China Sea shelf, as reported in previous studies (Liu et al., 2010; Wang et al., 2009, 2010; Zheng et al., 2010). In contrast, pyrrhotite is the dominant magnetic mineral in sediments near the mouths of western Taiwan's rivers (Fig. 4d–f). Such a distinction is due to lithological difference between the catchments on both sides of the Taiwan Strait. The main rivers in western Taiwan (including the Choshui, Wu, Dachia and Daan, but excluding the Danshui in the north; see Fig. 1) are sourced from the montane areas underlain by metamorphic rocks that contain pyrrhotite (Horng and Roberts, 2006). In contrast to Taiwan's metamorphic terrains are the magnetite-bearing granitic and basaltic rock substrates in southeastern China where pyrrhotite has not been found. The difference between the two shores in the composition of magnetic minerals provides an excellent condition for using magnetic parameters as tracers to study sediment provenance and transport in the Taiwan Strait.

SEM observations with EDS analyses on magnetic extracts further confirm that detrital pyrrhotite and magnetite are respectively the dominant magnetic minerals on the east and west sides of the Taiwan Strait (Fig. 5). It can also be noted in Fig. 5 that pyrrhotite grains sourced from western Taiwan are larger and less well sorted than those of magnetite derived from southeastern China. Considering that the hardness and stability of pyrrhotite are no greater than that of magnetite, this difference indicates that sediments from Taiwan experienced more rapid transport from source to sink due to steep topography and frequent floods associated with typhoons or intense rainfalls. As such, the pyrrhotite grains are rugged and poorly sorted. Subsequent to the "sloppy" deposition of fluvial sediments near western Taiwan, portions of these pyrrhotite-bearing sediments can be transported to the Kuan-Yin Depression, as indicated by the XRD analysis of surface sediments (Fig. 4c).

4.2. Magnetic features of surface sediments in the Taiwan Strait

More information about the source-to-sink dispersal of sediments in the Taiwan Strait can be gleaned from an integrated evaluation of magnetic properties of surface sediments. Given in Fig. 6a–e are plots showing correlations between various magnetic parameters. These plots can be based upon to characterize the concentration, composition, and granulometry of magnetic minerals contained in the sediment samples. To facilitate the following discussion, the data points in Fig. 6 are divided into six groups based on their provenances and magnetic features: (1) sediments from western Taiwan (the WT group (circles), which is further separated into WT-1 (in blue), WT-2 (in black), and WT-3 (in green) subgroups based on more detailed magnetic properties), (2) sediments from southeastern China (the SEC group; red triangles), (3) sediments from northern Taiwan (the NT group; light blue squares), (4) reworked relict sediments from Taiwan Shoal and Penghu Archipelago (the TS group; pink diamonds), (5) fluvial sediments of western Taiwan (the FSWT group (stars), which is further divided into subgroups FSWT-1 (in gray; for sediments from rivers' upper reaches) and FSWT-2 (in brown; for sediments from river mouths), and (6) fluvial sediments near the mouths of southeastern China rivers (the FSSEC group; yellow stars). To better view and interpret the data from a geographic perspective, the locations of the data points shown in Fig. 6a–e are mapped out in Fig. 6f, with numbers assigned to the data or sampling points to indicate their rankings in mass-specific magnetic susceptibility (χ) within each group or subgroup. Magnetic properties of all groups and subgroups are summarized in Table 1 and the data for all samples can be found in their entirety at http://dmc.earth.sinica.edu.tw/Contributor/Horng/mag2011/Magnetic_properties_TS.xls.

It is evident from Fig. 6a–d and Table 1 that, excluding the WT-2 and WT-3 subgroups, the values of χ, SIRM and HIRM in the WT-1 subgroup are generally lower than those in the SEC group, indicating that the WT-1 subgroup has "softer" magnetic minerals in much lower concentration compared with the SEC group. Another distinction between them is that the SEC group has smaller S-ratio in a narrow range (82.2% to 84.9%). Integrating these magnetic properties with XRD and SEM observations, we conclude that the magnetic minerals in the WT-1 subgroup are pyrrhotite and magnetite in rather low concentrations due to dilution by higher fluxes of non-magnetic materials from western Taiwan rivers.

It is also clear from Fig. 6a–d that, except two data points of the FSWT-2 subgroup (labeled 1 and 2 from the northern Danshui and Fengshan Rivers, respectively), the magnetic properties of this subgroup are quite similar to those of the FSWT-1 subgroup. This indicates that the magnetic features of sediments at the mouths of western Taiwan rivers are mainly derived from the metamorphic terrains in the rivers' upper reaches, with very minor contribution from sedimentary rocks and soils in the western foothills or elsewhere. However, it should be noted that the total data points of the FSWT group deviate from those in the WT-1 subgroup and show larger scatter in the values of magnetic parameters, particularly for the data point labeled 1 in the insets. Such variations found in the FSWT group reflect not only very dynamic condition at the rivers' mouths but also diverse geology of the drainage basins (to be further discussed later). Once fluvial sediments are discharged into the sea, hydrodynamic processes will homogenize sediments and reduce the variation in magnetic properties, as shown for the WT-1 subgroup in Fig. 6. However, the WT-2 and WT-3 subgroups have magnetic properties very different from those of the WT-1 subgroup.

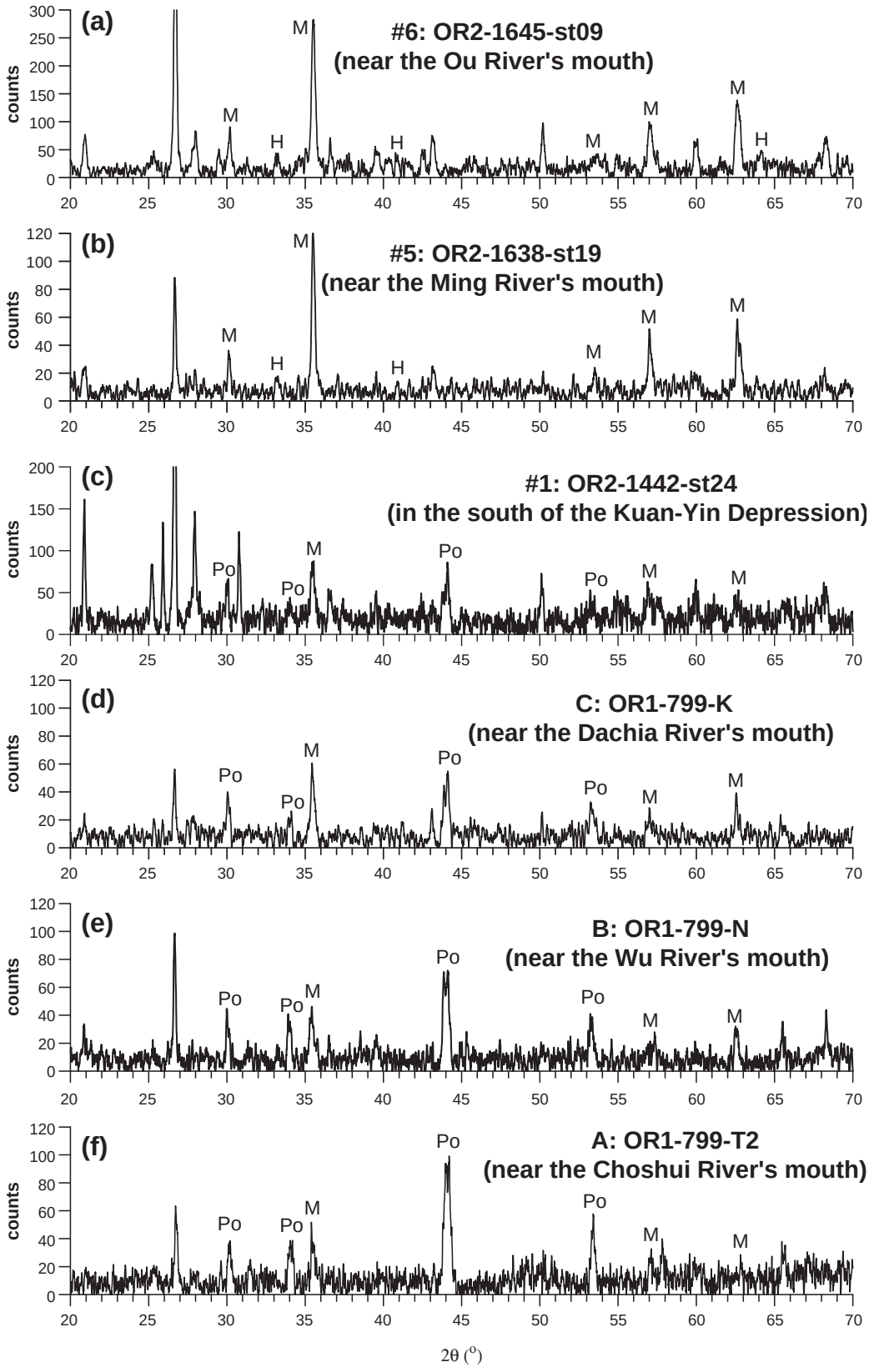

Fig. 4. X-ray diffractograms of magnetic extracts from surface sediments collected from six representative sites in the Taiwan Strait. They are located (a–b) near the mouths of the Ou and Ming Rivers in southeastern China, (c) in the south of the Kuan-Yin Depression, and (d–f) near the mouths of Dachia, Wu and Choshui Rivers off western Taiwan. Magnetite (M), accompanied by a small amount of hematite (H), is the dominant magnetic mineral in sediments delivered by the Ou and the Ming Rivers whereas pyrrhotite (Po), which has never been found in Chinese rivers, is more abundant than magnetite in Taiwan's fluvial sediments. The six sites are marked by crossed dots in Fig. 1 and labeled by #6, #5, #1, C, B, and A from the northwest toward the southeast.

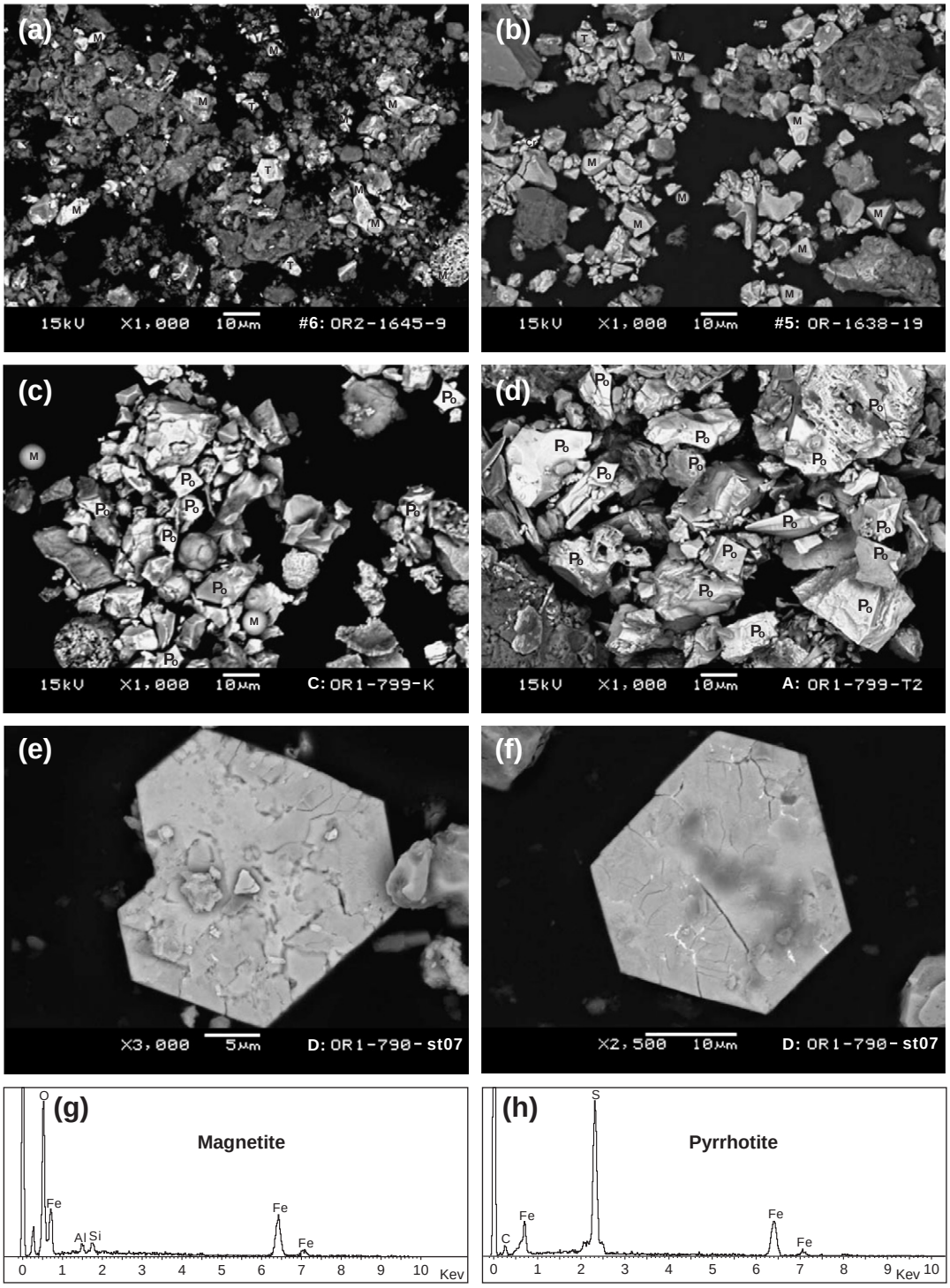

Fig. 5. (a–d) SEM images of magnetic extracts from surface sediments near the mouths of Ou, Ming, Dachia, and Choshui Rivers, respectively (sites #6, #5, C and A in Fig. 1). These images are in the same scale (×1000) and show that the grain sizes of magnetite (M) or titanomagnetite (T) from southeastern China are smaller than those of pyrrhotite (Po) from western Taiwan. Some anthropogenic magnetic spherules derived from air pollution products (Horng et al., 2009) can also be found in the samples. (e–f) Hexagonal outline of pyrrhotite crystals from a sediment core (OR1-790-st07; site D in Fig. 1) at the northwest of Daan River's mouth. (g–h) EDS spectra of magnetite and pyrrhotite. Note that, unlike XRD analysis (Fig. 4), hematite cannot be discriminated from magnetite by SEM and EDS analyses.

The magnetic behaviors of the WT-2 subgroup (i.e., 3 surface samples near the mouth of the Choshui River, see Fig. 6f) are almost the same as those in the FSWT group, suggesting that the sediments were freshly exported fluvial material not yet modified by marine processes. As regards the WT-3 subgroup, it is characterized by the lowest values of χ, SIRM, HIRM, and the S-ratio among all types of surface sediments (Fig. 6), indicating the lowest concentration of magnetic minerals in this subgroup. Samples of this subgroup generally contain a larger fraction of coarse-grained (>63 μm) sediment and are mainly distributed near the mouths of western Taiwan's rivers or along the coast (Fig. 6f). On the other hand, the FSSEC group extends the linear trend defined by the SEC group to higher values on the SIRM vs. χ plot (Fig. 6a), suggesting that it is a major source for the SEC group. Mixing of this endmember with sediments in the WT-1 subgroup by hydrodynamic processes can account for the dominant trends seen in Fig. 6a–d.

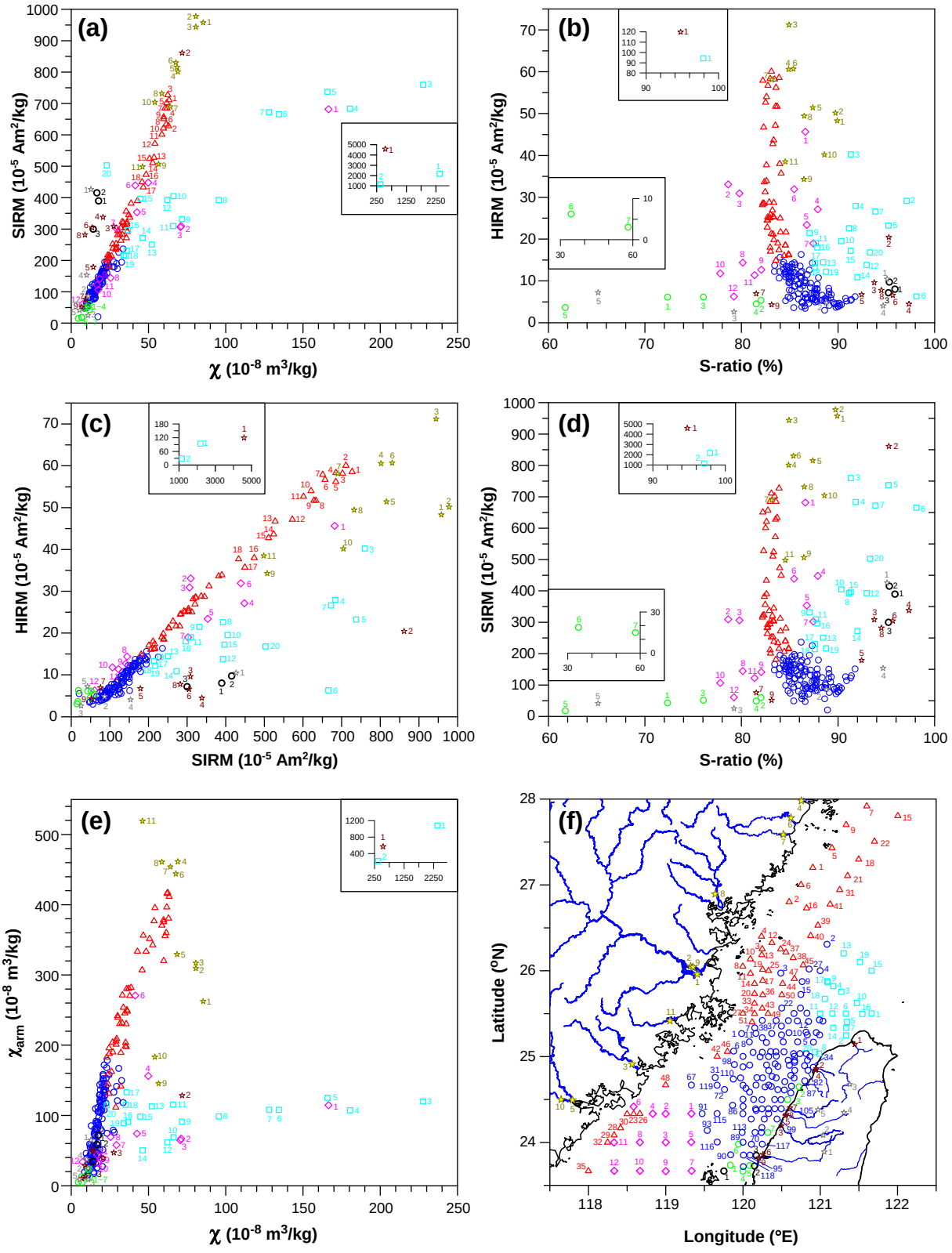

Fig. 6. Plots showing correlation between various magnetic properties in surface sediments of the Taiwan Strait: (a) SIRM vs. χ, (b) HIRM vs. the S ratio, (c) HIRM vs. SIRM, (d) SIRM vs. the S ratio, (e) χ_{arm} vs. χ, and (f) spatial distribution (latitude vs. longitude) of the sampling sites. The insets in (a) through (e) show outliers that cannot be covered in the main plots. Different colors and symbols are used to distinguish sediment provenances with diverse magnetic properties as described in the text. Numbers next to the symbols indicate the rankings of χ for each sample in various provenances. All these data can be found in their entirety in the Appendix to the online version of this article and also at: http://dmc.earth.sinica.edu.tw/Contributor/Horng/mag2011/Magnetic_properties_TS.xls.

In contrast to the WT-3 subgroup, the NT group shows the highest concentrations of magnetic minerals among the four groups of surface sediments in the Taiwan Strait. Sediments of this group are mainly derived from the Danshui River whose upper reaches drain metamorphic terrains (Fig. 1). However, due to the very low-grade metamorphism (i.e., prehnite-pumpellyite facies), pyrrhotite is absent in the

Table 1
A summary of measured values of magnetic parameters (χ, SIRM, HIRM, the S-ratio, χ_{arm}, and χ_{arm}/χ) for surface sediments (WT, SEC, NT, and TS groups) in the Taiwan Strait and fluvial sediments from western Taiwan and southeastern China (FSWT and FSSEC groups, respectively).

		FSWT-1 subgroup (n=5)	FSWT-2 subgroup (n=9)	WT-1 subgroup (n=123)	WT-2 subgroup (n=3)	WT-3 subgroup (n=7)	FSSEC group (n=11)	SEC group (n=51)	NT group (n=20)	TS group (n=12)
χ	Range	5.4 – 12.8	6.7 – 538.4	8.6 – 33.5	14.1 – 17.6	4.5 – 11.8	46.1 – 85.3	22.9 – 63.3	23.0 – 2378.0	7.4 – 166.5
(10^{-8} m^3/kg)	Mean ± s. d.	10.0 ± 2.8	79.1 ± 173.4	17.6 ± 4.8	16.1 ± 1.8	8.7 ± 2.8	66.5 ± 12.3	40.4 ± 13.4	212.8 ± 516.8	46.4 ± 43.1
SIRM	Range	25.2 – 426.5	51.7 – 4584.0	20.1 – 236.1	299.7 – 415.2	14.9 – 59.7	498.4 – 977.8	181.2 – 727.0	214.2 – 2180.0	60.6 – 681.7
(10^{-5} Am^2/kg)	Mean ± s. d.	146.6 ± 164.2	774.9 ± 1447.6	125.3 ± 40.5	368.1 ± 60.6	36.2 ± 18.7	769.2 ± 164.6	391.6 ± 169.9	553.1 ± 453.1	284.6 ± 181.6
HIRM	Range	2.6 – 10.5	4.4 – 119.9	3.0 – 16.3	7.2 – 9.7	3.1 – 6.2	34.3 – 71.2	14.9 – 60.1	6.3 – 94.4	6.3 – 45.7
(10^{-5} Am^2/kg)	Mean ± s. d.	5.9 ± 3.1	20.8 ± 37.5	8.4 ± 3.4	8.3 ± 1.3	5.0 ± 1.3	51.2 ± 11.0	32.9 ± 14.5	23.1 ± 18.4	22.3 ± 11.7
S-ratio	Range	65.2 – 95.1	81.5 – 97.3	83.4 – 91.8	95.2 – 95.9	34.4 – 82.0	83.1 – 89.9	82.2 – 84.9	87.0 – 98.1	77.8 – 87.9
(%)	Mean ± s. d.	84.6 ± 12.6	92.0 ± 5.7	86.8 ± 1.9	95.5 ± 0.4	66.6 ± 16.9	86.5 ± 2.2	83.3 ± 0.7	91.6 ± 3.5	82.8 ± 3.8
χarm	Range	8.7 – 65.1	10.3 – 569.7	13.7 – 178.2	34.2 – 72.0	4.5 – 23.8	145.5 – 519.2	111.5 – 417.1	50.4 – 1080.0	32.0 – 270.7
($10^{-8}$$m^3$/kg)	Mean ± s. d.	29.0 ± 23.5	103.3 ± 178.3	84.7 ± 44.5	55.0 ± 19.2	13.2 ± 7.6	353.4 ± 123.9	269.6 ± 86.2	155.3 ± 220.2	85.0 ± 68.6
χ_{arm}/χ	Range	0.8 – 5.1	1.1 – 3.8	1.2 – 8.1	2.4 – 4.1	0.7 – 2.1	2.6 – 11.3	3.9 – 8.2	0.5 – 5.0	0.7 – 6.5
	Mean ± s. d.	2.7 ± 1.7	2.2 ± 1.0	4.6 ± 1.8	3.4 ± 0.9	1.5 ± 0.6	5.6 ± 2.6	6.7 ± 0.9	1.7 ± 1.2	2.5 ± 1.7

Notes: (1) The four primary groups of surface sediments in the Taiwan Strait are identified by their respective provenances as western Taiwan (WT), southeastern China (SEC), northern Taiwan (NT), and the Taiwan Shoal (TS). The WT group is further divided into three subgroups (WT-1, WT-2, and WT-3) based on more detailed magnetic properties. (2) The FSWT group is divided into two subgroups (FSWT-1 and FSWT-2) to represent sediments from the rivers' upper reaches and mouths, respectively. (3) n: number of samples in each group or subgroup; s. d.: standard deviation.

parent rocks and its weathering products. Therefore, magnetite eroded from the Plio–Pleistocene Tatun and Chilung volcanic groups becomes the dominant magnetic mineral in fluvial sediments in the lower reaches of the Danshui River (Fig. 1). This results in prominent values of magnetic parameters for the fluvial sediments collected at the mouth of the Danshui River (i.e., the data point labeled 1 for the FSWT-2 subgroup in Fig. 6a–d) and very high concentrations of magnetite in the NT group.

As shown in Fig. 6a–d, the magnetic properties of the TS group, characterized by quite low values in the S-ratio (77.8% to 87.9%) and rather large variations in magnetic concentrations, are different from those groups described above. Samples of the TS group are located to the north of Taiwan Shoal and the northwest of Penghu Archipelago covered by coarse-grained relic sediments and debris of basaltic rocks, respectively (Boggs et al., 1979). Conceivably, sediments of the TS group are sourced from these two adjoining regions. The lower χ_{arm}/χ values for the NT and TS groups (Fig. 6e and Table 1) also indicate that sediments of these two groups have significantly larger grain size than those of other groups. Thus, in the preparation of cubic samples for these two groups, it was necessary to use >63 μm nets.

4.3. Hydrodynamically modulated distribution of magnetic properties in surface sediments

Based on magnetic properties elaborated above, at least four source regions can be identified for sediments in the Taiwan Strait, which are western Taiwan, southeastern China, northern Taiwan, and the Taiwan Shoal. The source-to-sink dispersal of sediments can be delineated from the distribution of magnetic properties shown in Fig. 7a–e. Sediments sourced from western Taiwan are discharged largely toward the Chang-Yun Ridge and the Kuan-Yin Depression (Figs. 1 and 2), and are characterized by lower χ, SIRM and HIRM values and more variable S-ratio. In contrast, sediments derived from southeastern China show higher χ, SIRM and HIRM values and a narrow range of the S-ratio (82.2% to 84.9%). These sediments are transported southward primarily by the China Coastal Current and are confined in the mud clinoform stretching from the Yangtze River's mouth toward the north of the Wu-Chiu Depression (Liu et al., 2007, 2008; Xu et al., 2009).

The other two dispersal systems are much smaller in scale. Sediments delivered from the northern Taiwan by the Danshui and Fengshan Rivers have the highest χ, SIRM, HIRM, and the S-ratio. They are deposited in the northeastern peripheries of the Kan-Yin Depression. Lastly, sediments from Taiwan Shoal and Penghu Archipelago are rather high in χ, SIRM and HIRM, but quite low in the S-ratio (77.8% to 87.9%), which are distributed in the southern part of the Wu-Chiu Depression.

Besides magnetic properties described above, the distribution of sediment grain size, as shown in Fig. 7e, also manifests the transport pathways and sedimentation processes of sediments under the influence of hydrodynamics in the Taiwan Strait (Figs. 2 and 3). For instance, the coarse-grained sediments distributed in the eastern Chang-Yun Ridge, the southern part of the Wu-Chiu Depression, and the northeastern edge of the Kan-Yin Depression are not only affected by the prevailing currents but also by the strong tidal currents there. The magnetic granulometry of surface sediments inferred from the χ_{arm}/χ values is consistent with the grain size distribution shown in Fig. 7f (Huh et al., 2011).

4.4. Temporal variability of magnetic properties revealed from dated cores

Besides surface sediments, a large number of sediment cores were collected throughout the Taiwan Strait during 2005–2010. In order to unravel temporal variability in magnetic properties, six cores were selected for this study. These six cores were chosen based on two critical criteria. First, they provide the best sediment chronology, with concordant sedimentation rates derived from ^{210}Pb and ^{137}Cs (Huh et al., 2011). Secondly, these cores, identified by #1–#6 in Fig. 1, occupy key locations with respect to source-to-sink pathways of sediments in the Taiwan Strait. As summarized in Huh et al. (2011), these 6 core sites are located at various segments of three sediment dispersal systems. Core #1, located near the Dachia and the Wu Rivers' mouths, belongs to the system derived from western Taiwan rivers (including the Choshui River as the southernmost one) which empty directly into the Kan-Yin Depression. Core #2, on the path of the western (deep) branch of the Kuroshio Branch Current, belongs to another system derived from Taiwan's southwestern rivers (Fig. 2). On the other side of the strait are core #5 near the Ming River's mouth and core #6 near the Ou River's mouth; both are on the path of the China Coastal Current. In-between the two shores are cores #3 and #4 at the confluence of the dispersal systems from Taiwan and mainland China.

Fig. 8a–c show the time series of χ, SIRM, and HIRM derived from the above-mentioned cores. At essentially all times, the lowest χ, SIRM, and HIRM were found in core #1, and the highest in core #6. The values of χ are very close between cores #1 and #2, and between cores #5 and #6, but obviously different between cores #3 and #4. It is worthwhile noting that χ in cores #3 and #4 decreases with time, suggesting a steady increase of sediment supply from Taiwan.

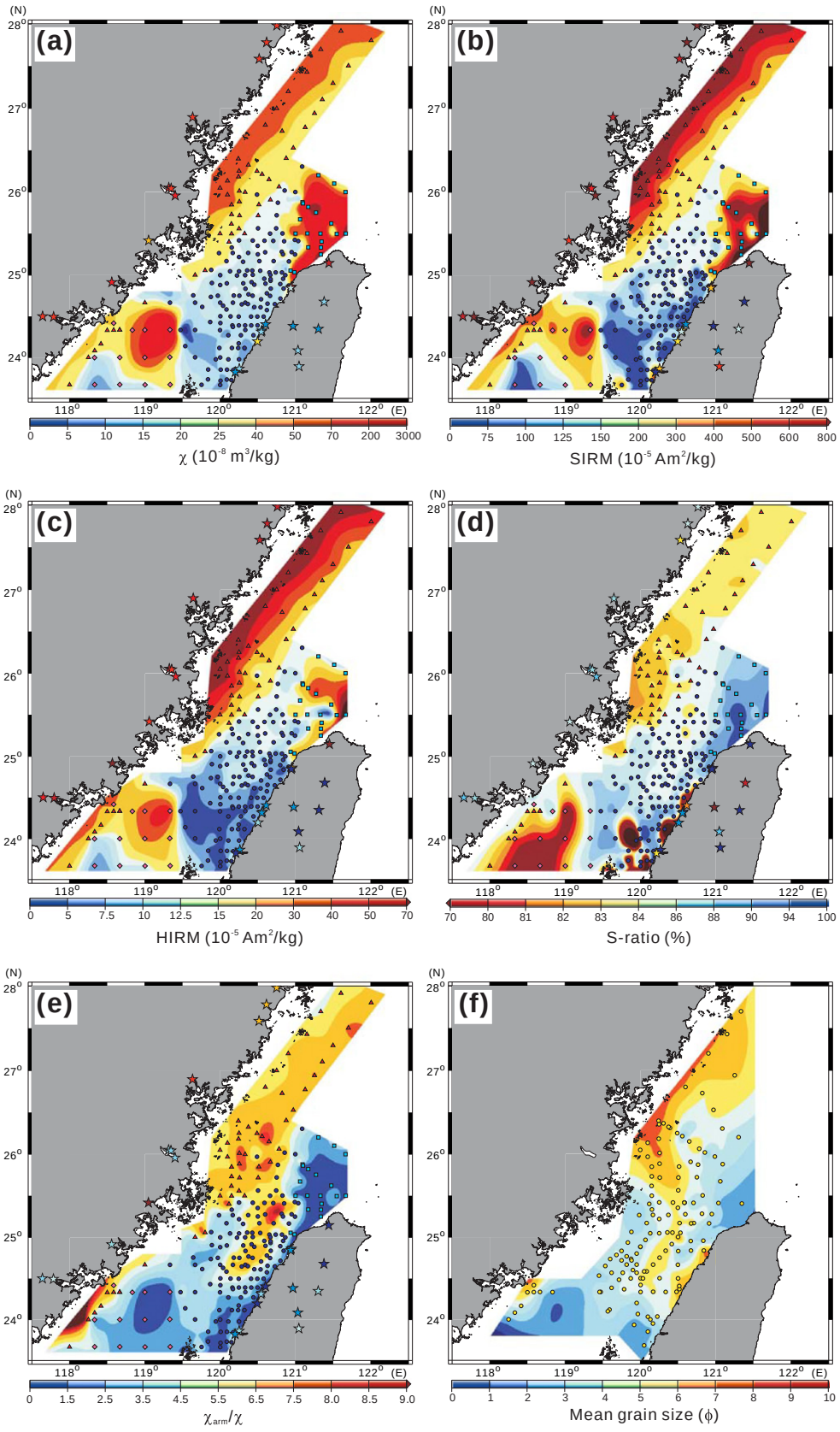

Fig. 7. Spatial distribution of various magnetic properties and mean grain size in surface sediments of the Taiwan Strait: (a) χ, (b) SIRM, (c) HIRM, (d) the S-ratio, (e) the χ_{arm}/χ ratio, and (f) mean grain size (redrawn from Huh et al., 2011). Different colors and symbols (blue dots, red triangles, light blue squares, and pink diamonds) are used to distinguish four sediment provenances (i.e., western Taiwan, southeastern China, northern Taiwan, and the Taiwan Shoal, respectively). The stars representing fluvial sediments collected from western Taiwan and southeastern China are also shown in color to reveal their magnetic properties.

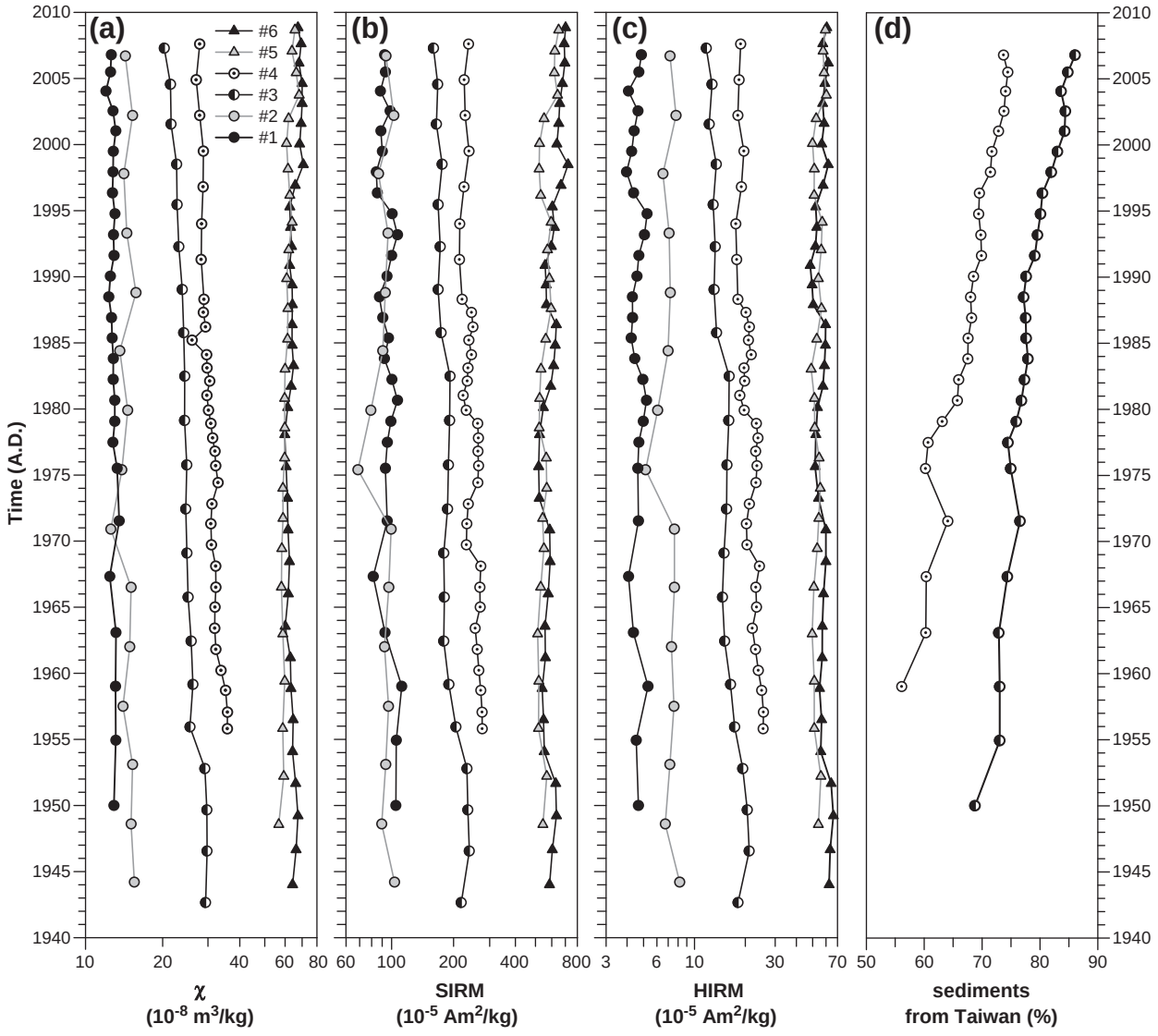

Fig. 8. (a–c) Downcore variations of magnetic properties (χ, SIRM, and HIRM; in logarithmic scale) of six well-dated cores (#1–#6, locations indicated in Fig. 1), and (d) the change with time of Taiwan's contribution to sediments deposited in two cores (#3 and #4) in the middle of the Taiwan Strait, as calculated using a two-endmember mixing model. Sediment chronology was derived from ^{210}Pb and ^{137}Cs profiles (Huh et al., 2011).

Assuming sediments at the sites of cores #3 and #4 are mixtures of sediments from core sites #1 and #6 and using their time-variable χ as endmember values, we calculated that sediment supply from Taiwan has increased ~18% in the past 5–6 decades (Fig. 8d), which may very well be related to land development and increased frequency of intense rainfalls in Taiwan during this period (Liu et al., 2009).

5. Conclusions

In this study we have demonstrated that magnetic properties of pyrrhotite-bearing sediments from the metamorphic terrains in Taiwan are utterly different from those of magnetite-bearing sediments derived from the igneous terrains in southeastern China. Based on the sharp distinction, we have investigated the provenances and source-to-sink pathways of sediments in the Taiwan Strait. Although magnetite has long been considered as the most common magnetic mineral in various rocks and sediments, the occurrence of pyrrhotite as an accessory mineral in orogenic belts subject to regional metamorphism has been increasingly documented (Carpenter, 1974; Itaya, 1975; Rochette, 1987; Schill et al., 2002). This may have far-reaching implications for studying source-to-sink systems around the world and through time. Milliman and Meade (1983) estimated that rivers with sediment loads greater than ~15×10^6 ton/year contribute about 7×10^9 tons of suspended sediment to the world oceans annually. Of this worldwide total land-to-sea sediment discharge, about 70% is from southern Asia and mountainous islands in the Pacific and Indian Oceans, where sediment yields are the highest (Milliman and Syvitski, 1992). It is worthwhile noting that, like the case of Taiwan, most small mountainous rivers in the circum-Pacific islands are sourced from exhumed metamorphic terrains that very probably contain pyrrhotite. The rapid and massive transport of sediments from these islands is favorable for the preservation and burial of pyrrhotite at the seafloor. It is thus proposed that pyrrhotite can be a unique tracer for studying source-to-sink dispersal of sediments originated from small mountainous rivers draining metamorphic terrains in the Pacific rim.

Acknowledgments

We are grateful to Kuo-Hang Chen and Chun-Hung Lin for their assistance in sample processing and analysis in the laboratory and the preparation of figures. Dr. Zhifei Liu of Tongji University generously provided fluvial sediments of southeastern China for this work. Two

anonymous reviewers made comments and suggestions that improved this paper. This work is supported by the Institute of Earth Sciences, Academia Sinica and National Science Council grants NSC99-2116-M-001-019 (to CSH) and NSC97-2611-M-001-002-MY3 (to CAH).

Appendix A. Supplementary data

Supplementary data to this article can be found online at doi:10.1016/j.epsl.2011.07.002.

References

Banerjee, S.K., King, J.W., Marvin, J., 1981. A rapid method for magnetic granulometry with applications to environmental studies. Geophys. Res. Lett. 8, 333–336.
Boggs, S., Wang, W.-C., Lewis, F.S., Chen, J.-C., 1979. Sediment properties and water characteristics of the Taiwan shelf and slope. Acta Oceanogr. Taiwanica 10, 10–49.
Carpenter, R.H., 1974. Pyrrhotite isograd in southeastern Tennessee and southwestern North Carolina. Geol. Soc. Am. Bull. 85, 451–456.
Chen, C.-H., Ho, H.-C., Shea, K.-S., Lo, W., Lin, W.-H., Chang, H.-C., Huang, C.-S., Lin, C.-W., Chen, G.-H., Yang, C.-N., Lee, Y.-H., 2000. Geological map of Taiwan. Central Geological Survey. Ministry of Economic Affairs, Republic of China.
Dadson, S.J., Hovius, N., Chen, H., Dade, W.B., Hsieh, M.-L., Willett, S.D., Hu, J.-C., Horng, M.-J., Chen, M.-C., Stark, C.P., Lague, D., Lin, J.-C., 2003. Links between erosion, runoff variability and seismicity in the Taiwan orogen. Nature 426, 648–651.
Evans, M.E., Heller, F., 2003. Environmental magnetism: principles and applications of enviromagnetics. Academic Press, San Diego. 299 pp.
Horng, C.-S., Roberts, A.P., 2006. Authigenic or detrital origin of pyrrhotite in sediments?: Resolving a paleomagnetic conundrum. Earth Planet. Sci. Lett. 241, 750–762.
Horng, C.-S., Huh, C.-A., Chen, K.-H., Huang, P.-R., Hsiung, K.-H., Lin, H.-L., 2009. Air pollution history elucidated from anthropogenic spherules and their magnetic signatures in marine sediments offshore of Southwestern Taiwan. J. Mar. Syst. 76, 468–478.
Huh, C.-A., Lin, H.-L., Lin, S., Huang, Y.-W., 2009. Modern accumulation rates and a budget of sediment off the Gaoping (Kaoping) River, SW Taiwan: a tidal and flood dominated depositional environment around a submarine canyon. J. Mar. Syst. 76, 405–416.
Huh, C.-A., Chen, W.-F., Hsu, F.-H., Su, C.-C., Chiu, J.-K., Lin, S., Liu, C.-S., Huang, B.-J., 2011. Modern (<100 years) sedimentation in the Taiwan Strait: rates and source-to-sink pathways elucidated from radionuclides and particle size distribution. Cont. Shelf Res. 31, 47–63.
Itaya, T., 1975. Pyrrhotite from the Sanbagawa pelitic schists of the Shiraga-yama area, central Shikoku. Jpn. Mineral. J. 8, 25–37.
Jan, S., Wang, J., Chern, C.-S., Chao, S.-Y., 2002. Seasonal variation of the circulation in the Taiwan Strait. J. Mar. Syst. 35, 249–268.
Jan, S., Chern, C.-S., Wang, J., Chao, S.-Y., 2004. The anomalous amplification of M2 tide in the Taiwan Strait. Geophys. Res. Lett. 31, L07308.
Jan, S., Sheu, D.D., Kuo, H.-M., 2006. Water mass and through flow transport variability in the Taiwan Strait. J. Geophys. Res. 111, C12012.
King, J.W., Channell, J.E.T., 1991. Sedimentary magnetism, environmental magnetism, and magnetostratigraphy. U.S. National Report to International Union of Geodesy and Geophysics 1987–1990. Rev. Geophys. 29, 358–370.
Lee, H.-J., Chao, S.-Y., 2003. A climatological description of circulation in and around the East China Sea. Deep Sea Res. Part II 50, 1065–1084.
Li, Y.-H., 1976. Denudation of Taiwan Island since the Pliocene Epoch. Geology 4, 105–107.
Liao, H.-R., Yu, H.-S., Su, C.-C., 2008. Morphology and sedimentation of sand bodies in the tidal shelf sea of eastern Taiwan Strait. Mar. Geol. 248, 161–178.
Liu, J.-P., Xu, K.-H., Li, A.-C., Milliman, J.D., Velozzi, D.M., Xiao, S.-B., Yang, Z.-S., 2007. Flux and fate of Yangtze River sediment delivered to the East China Sea. Geomorphology 85, 208–224.
Liu, J.-P., Liu, C.-S., Xu, K.-H., Milliman, J.D., Chiu, J.-K., Kao, S.-J., Lin, S.-W., 2008. Flux and fate of small mountainous rivers derived sediments into the Taiwan Strait. Mar. Geol. 256, 65–76.
Liu, S.-C., Fu, C.-B., Shiu, C.-J., Chen, J.-P., Wu, F.-T., 2009. Temperature dependence of global precipitation extremes. Geophys. Res. Lett. 36, L17702.
Liu, S.-M., Zhang, W.-G., He, Q., Li, D.-J., Liu, H., Yu, L.-Z., 2010. Magnetic properties of East China Sea shelf sediments off the Yangtze Estuary: influence of provenance and particle size. Geomorphology 119, 212–220.
Ma, L.-F. (Ed.), 2002. Geological Atlas of China. The Geological Publishing House, Beijing. 348 pp.
Maher, B.A., Thompson, R. (Eds.), 1999. Quaternary Climates, Environments and Magnetism. Cambridge University Press, Cambridge. 390 pp.
Milliman, J.D., Meade, R.H., 1983. World-wide delivery of river sediment to the oceans. J. Geol. 91, 1–21.
Milliman, J.D., Syvitski, J.P.M., 1992. Geomorphic/tectonic control of sediment discharge to the ocean: the importance of small mountainous rivers. J. Geol. 100, 525–544.
Oldfield, F., 1999. The rock magnetic identification of magnetic mineral and grain size assemblages. In: Walden, J., Oldfield, F., Smith, J. (Eds.), Environmental Magnetism: A Practical Guide. : Technical Guide, 6. Quaternary Research Association, London, pp. 98–112.
Rochette, P., 1987. Metamorphic control of the magnetic mineralogy of black shales in the Swiss Alps: toward the use of "magnetic isograde". Earth Planet. Sci. Lett. 84, 446–456.
Schill, E., Appel, E., Gautam, P., 2002. Towards pyrrhotite/magnetite geothermometry in low-grade metamorphic carbonates of the Tethyan Himalayas (Shiar Khola, Central Nepal). J. Asian Earth Sci. 20, 195–201.
Thompson, R., Oldfield, F., 1986. Environmental Magnetism. Allen & Unwin, London. 227 pp.
Wang, Y.-H., Jan, S., Wang, D.-P., 2003. Transports and tidal current estimates in the Taiwan Strait from shipboard ADCP observations (1999–2001). Estuarine Coastal Shelf Sci. 57, 193–199.
Wang, Y.-H., Yu, Z.-G., Li, G.-X., Oguchi, T., He, H.-J., Shen, H.-T., 2009. Discrimination in magnetic properties of different-sized sediments from the Changjiang and Huanghe Estuaries of China and its implication for provenance of sediment on the shelf. Mar. Geol. 260, 121–129.
Wang, Y.-H., Dong, H.-L., Li, G.-X., Zhang, W.-G., Oguchi, T., Bao, M., Jiang, H.-C., Bishop, M.E., 2010. Magnetic properties of muddy sediments on the northeastern continental shelves of China: implication for provenance and transportation. Mar. Geol. 274, 107–119.
WRB (Water Resources Bureau), 1997. Hydrological Year Book of Taiwan. Ministry of Economic Affairs. 378 pp.
Wu, C.-R., Chao, S.-Y., Hsu, C., 2007. Transient, seasonal and interannual variability of the Taiwan Strait current. J. Oceanogr. 63, 821–833.
Xu, K.-H., Milliman, J.D., Li, A.-C., Liu, J.P., Kao, S.-J., Wan, S.-M., 2009. Yangtze- and Taiwan-derived sediments on the inner shelf of East China Sea. Cont. Shelf Res. 29, 2240–2256.
Yang, S.-L., Zhao, Q.-Y., Belkin, I.M., 2002. Temporal variation in the sediment load of the Yangtze river and the influences of human activities. J. Hydrol. 263, 56–71.
Yang, S.-L., Belkin, I.M., Belkina, A.I., Zhao, Q.-Y., Zhu, J., Ding, P.-X., 2003. Delta response to decline in sediment supply from the Yangtze River: evidence of the recent four decades and expectations for the next half-century. Estuarine. Coastal. Shelf Sci. 57, 689–699.
Zheng, Y., Kissel, C., Zheng, H.-B., Laj, C., Wang, K., 2010. Sedimentation on the inner shelf of the East China Sea: magnetic properties, diagenesis and paleoclimate implications. Mar. Geol. 268, 34–42.